LONGITUDINAL AND TRANSVERSE DISPERSION IN POROUS MEDIA BY PORE-SCALE MODELING AND CONTINOUS TIME RANDOM WALK (CTRW) THEORY

BRANKO BIJELJIC, MARTIN J. BLUNT
Department of Earth Science & Engineering, Imperial College, Exhibition Road, London, SW7 2AZ, UK, Email: b.bijeljic@imperial.ac.uk

ABSTRACT

We provide a physically-based explanation for the complex macroscopic behavior of longitudinal and transverse dispersion in porous media as a function of Peclet number, *Pe*. A Lagrangian pore-scale transport model incorporating flow and molecular diffusion is applied in lattices of throats with square cross-section whose characteristics are representative of Berea sandstone. The model accurately predicts NMR, laser fluorescence and breakthrough data for the experimental dependence of the longitudinal dispersion coefficient, D_L, on *Pe*. We compute the probability, $\psi(t)dt$ that a particle moves from one throat junction to a nearest neighbor junction in the time interval t to $t+dt$ and fit it to a simple analytical expression that depends on the mean advective transit time, a late-time diffusive cut-off and a parameter β characterizing the distribution of transit times between pores. Then, interpreting transport as a continuous time random walk (CTRW), we show: (1) that the power-law dispersion regime is controlled by the variation in average velocity between throats (the distribution of local *Pe* rather than by diffusion from boundary layers within throats), giving $D_L \sim Pe^{\delta_L}$ with $\delta_L = 3\text{-}\beta \approx 1.2$; (2) the cross-over to a linear regime for $D_L \sim Pe^{\delta_L}$ for $Pe > Pe^{crit} \approx 400$ is due to a transition from a diffusion-controlled late-time cut-off, to transport governed by advective movement; and (3) that the transverse dispersion coefficient $D_T \sim Pe$ for all $Pe >> 1$. We provide a quantitative description of both asymptotic and pre-asymptotic dispersion using CTRW with a physical interpretation of the parameters. Our demonstration that the power-law dependence of dispersion coefficient on *Pe* is due to the distribution of flow speeds in individual pores contrasts with the traditional theories of *Saffman* (1959) and *Koch and Brady* (1985).

1. INTRODUCTION

Solute transport in consolidated rocks is of central importance in the remediation of contaminated groundwater, radioactive waste disposal and tracer studies in oil recovery. In addition, solute mass transfer in beds of unconsolidated particles arises as an essential issue in the design of many industrial devices used for adsorption, chromatography, ion exchange, leaching and heterogeneous catalysis. Prediction of transport properties in both consolidated and unconsolidated porous media is difficult due to the highly complex geometry of the porous matrix. Solute must be transported throughout the porous medium for a time or length sufficiently large to allow for a full sampling of the flow field heterogeneity before the dispersion coefficient can reach an asymptotic value and the spreading becomes purely Gaussian. If these conditions are not satisfied, solute undergoes spreading in a pre-asymptotic regime for which the dispersion coefficient increases with time and the average distance

traveled [*Han et al.*, 1985; *Koch and Brady,* 1987; *Gelhar et al.*, 1992; *Sahimi*, 1995; *Berkowitz et al.*, 2000].

Furthermore, the behavior of the asymptotic dispersion coefficient as a function of Peclet number ($Pe = uL/D_m$, where u is the average flow speed, L is a characteristic length – the inter-pore distance or grain diameter – and D_m is the molecular diffusion coefficient) is surprisingly rich [*Pfannkuch,* 1963; *Bear,* 1988; *Dullien*, 1992; *Sahimi*, 1995; *Kandhai et al.*, 2002; *Khrapitchev and Callaghan*, 2003]. The longitudinal dispersion coefficient, D_L, is lower than D_m for $Pe \leq 1$ due to restricted diffusion imposed by the solid phase. With both diffusion and advection present ($Pe > 1$), there is a transition region to a power-law regime [*Sahimi*, 1995] where $D_L \sim Pe^{\delta_L}$ with $\delta_L \approx 1.2$ for experiments in beadpacks, sandpacks and homogeneous sandstones [*Pfannkuch,* 1963; *Sahimi*, 1995; *Bijeljic et al.*, 2004]. For $Pe > 400$ there is a cross-over to a purely advective, mechanical dispersion regime with $D_L \sim Pe$ [*Pfannkuch,* 1963; *Sahimi*, 1995; *Bijeljic et al.*, 2004]. For $Pe \gg 1$ *Saffman* [1959] and *Koch and Brady* [1985] predicted that $D_L \sim Pe\ln Pe$. The transverse dispersion coefficient, D_T, however, is lower than D_L and typically scales approximately linearly with Pe [*Fried* and *Combarnous*, 1971; *Sahimi*, 1995]. Despite numerous experimental and theoretical studies there is lack of fundamental understanding of how pore structure controls dispersion. In particular, there is no explanation of why an exponent $\delta_L = 1.2$ is obtained for intermediate Pe and why there is a transition to a linear regime at higher Pe.

Solute transport can be described as a continuous time random walk (CTRW) [*Scher and Lax*, 1973; *Berkowitz and Scher*, 1995; *Dentz et al.*, 2004]. Conceptually we can view transport as a series of steps as the solute moves between pores. Define $\psi(t)$ as the probability that a particle just arrived a pore will subsequently first reach a nearest neighbor pore after a time t. *Dentz et al.* [2004] suggested an empirical form for $\psi(t)$:

$$\psi(t) = A\left(1 + t/t_1\right)^{-(1+\beta)} e^{-t/t_2} \qquad (1)$$

where t_1 is the mean advective transit time, t_2 is a late-time cut-off and for $t_2 > t > t_1$ we see approximately power-law scaling with $\psi(t) \sim t^{-(1+\beta)}$ where β is a parameter characterizing the porous medium heterogeneity. The constant A is fixed by normalizing the probability to 1. Using Eq. (1) and CTRW analytical expressions for the movement of solute and the resultant dispersion coefficients can be derived that accurately match results of both field and laboratory-scale measurements using an appropriate value of β [*Levy and Berkowitz*, 2003; *Dentz et al.*, 2004]. We apply CTRW to transport at the pore scale and provide a physical interpretation of t_1, t_2 and β [*Bijeljic and Blunt*, 2006]. In CTRW $\psi(t)$ is the probability for a jump occurring; in this work we give a physical interpretation for the distance across which this jump occurs, namely between neighboring pores. This allows us to relate $\psi(t)$ to the macroscopic dispersion coefficient and to explain physically the dependence of D_L on Pe.

2. NETWORK MODEL OF DISPERSION

The algorithm for describing transport of a non-reactive tracer in porous media is:

1. Represent the porous medium with a network of pores and throats; 2. Calculate the mean velocity in each pore by invoking volume balance at each pore and solving the resultant series of linear equations numerically; 3. Use an analytic solution to determine the velocity profile in

each throat; 4. Inject particles into the network; 5. In each time step move particles in throats by advection and then diffusion; 6. At the throat walls use no-slip boundary conditions for advection and bounce-back boundary conditions for diffusion; 7. Impose rules for mixing at junctions (pores); 8. From the spatial distribution of particles in the network obtain dispersion coefficient at a given time.

We will briefly describe the most important features for understanding the model i.e. steps 1, 4, 7 and 8. For more detailed model description refer to *Bijeljic et al.* (2004).

Step 1 We represent the porous medium by mapping the pore-scale network obtained from reconstructed Berea sandstone (Fig. 1) [*Øren and Bakke, 2002*] to a two-dimensional diamond lattice of 60 by 60 pores consisting of 7320 throats of square cross-section. The mean throat radius is ~10μm, the average throat length is ~100μm, while the length of the network L_n in the flow direction and transverse to the flow direction is ~ 6mm. We use periodic boundary conditions that allow us to follow particle trajectories in the networks much larger than the L_n value above.

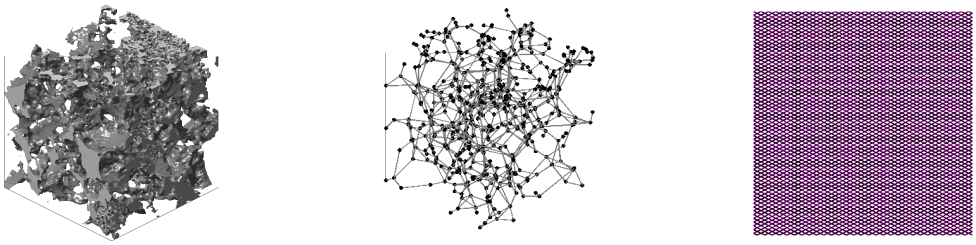

(a) (b) (c)

Fig. 1. Berea sandstone sample of size 3mm x 3mm x 3mm from *Øren and Bakke*, 2002 (a); A geologically equivalent network (b) and the diamond lattice network (c).

Step 4 Particles are injected simultaneously across the network so that their distribution is uniform in the direction transverse to the mean flow (when studying longitudinal dispersion) or is uniform in the flow direction (for transverse dispersion).

Step 7 We use both advective-based routing and complete mixing as the two limiting fluid mixing behaviors at pore junctions at large *Pe* and small *Pe* respectively. When a particle enters a pore in advective step we assign the outgoing throat according to the flow rate-weighted rule, that is the probability that the particle ends in a certain outgoing throat is proportional to the flow rate in the individual outgoing throat. When a particle enters a pore from a throat in diffusive step we assign the new throat according to an area-weighted rule, that is the probability that the particle enters a new throat is proportional to the cross-sectional area of the individual throat *i* (that can be the old throat, too).

Step 8 The longitudinal and transverse dispersion coefficients D_L and D_T are obtained by calculating the variance of the distance traveled by the particles in time *t*:

$$D_L = \frac{1}{2}\frac{d\sigma_L^2}{dt} \qquad D_T = \frac{1}{2}\frac{d\sigma_T^2}{dt} \quad . \tag{2}$$

3. RESULTS AND DISCUSSION

In this section we first present the comparison of both longitudinal and transverse asymptotic dispersion coefficients obtained from the pore scale network model with the experimental results. Furthermore, we show how our assumed truncated power-law probability function ψ of transit times between two neighboring pores (Eq. 1) accurately reproduces $\psi(\tau, Pe)$ obtained directly from the network simulations. Last but not least, we find an excellent agreement between the asymptotic longitudinal dispersion coefficients in the power-law regime, i.e. β=1.8 (Eq. 1) from the CTRW and δ_L = 3-β=1.2 (Eq. 1) from the network model and the experiments.

3.1 Longitudinal and transverse dispersion coefficient dependence on *Pe*

The model results for longitudinal dispersion (upper solid line) are plotted in Fig. 2 together with: a) the experimental data on unconsolidated bead packs obtained from breakthrough curves compiled by *Pfannkuch* (1963) (●), (b) data on bead packs obtained by Magnetic Resonance Imaging by *Seymour and Callaghan* (1997) (▲), *Kandhai et al.*, (2002) (■) and *Khrapitchev and Callaghan* (2003) (◆), (c) data on bead packs obtained by laser-induced fluorescence method by *Stöhr*, 2003 (▼) and (d) sandstone data in the low Peclet number limit (solid lines with bars [*Dullien*, 1992; *Legatski and Katz,* 1967*; Gist et al.,* 1997*; Frosch et al.,* 2003]. The model results for transverse dispersion (lower solid line in Fig. 2) are plotted together with: a) the experimental data on unconsolidated bead packs obtained from breakthrough curves (▽) [*Harleman, and Rumer*, 1963], (□) [*Hassinger and von Rosenberg*, 1968], (+) [*Gunn and Pryce*, 1969], and (○) [*Han et al.*, 1985], and (b) data on bead packs obtained by Magnetic Resonance Imaging by *Callaghan* and coworkers (×) [*Seymour and Callaghan*, 1997] and (Δ,◇) [*Khrapitchev and Callaghan*, 2003]. The data are plotted as dispersion coefficient divided by the molecular diffusion coefficient (D_L/D_m) and (D_T/D_m) versus Peclet number.

For longitudinal dispersion, in the absence of advection (low *Pe*), molecular diffusion is the only mechanism for fluid mixing. This diffusion is restricted as the porous medium matrix acts as a barrier to molecules, thus reducing the mean free path of molecules, which results in the ratio D_L/D_m being smaller than unity. We obtain D_L/D_m =0.25 for Pe = 0, which is in the range obtained by either conductivity or MRI measurements for sandstones, including Berea sandstone [*Dullien*, 1992; *Legatski and Katz*, 1967; *Gist et al*., 1997; *Frosch et al*., 2003).

The first effects of advection on the dispersion are observed at Pe=0.1. At Pe=10 advection starts to have a much more pronounced contribution on mixing but diffusion effects are still present. The best fit of our results to $D_L \sim Pe^{\delta_L}$ in the regime $10 < Pe < 400$ is with a power-law coefficient δ_L = 1.2 which agrees with the experimental results compiled by *Pfannkuch* (1963) and the experiments by *Kandhai et al.* (2002) and *Stöhr* (2003).

In the mechanical dispersion regime ($Pe > 400$) we obtain a linear dependence of longitudinal dispersion coefficient with Peclet number. This is a purely advective-dominated dispersion regime in which particles in the throats do not spend sufficiently long to allow them to move significantly by molecular diffusion. The agreement with *Pfannkuch's* data and the MRI study by *Khrapitchev and Callaghan* (2003) in this regime is very good.

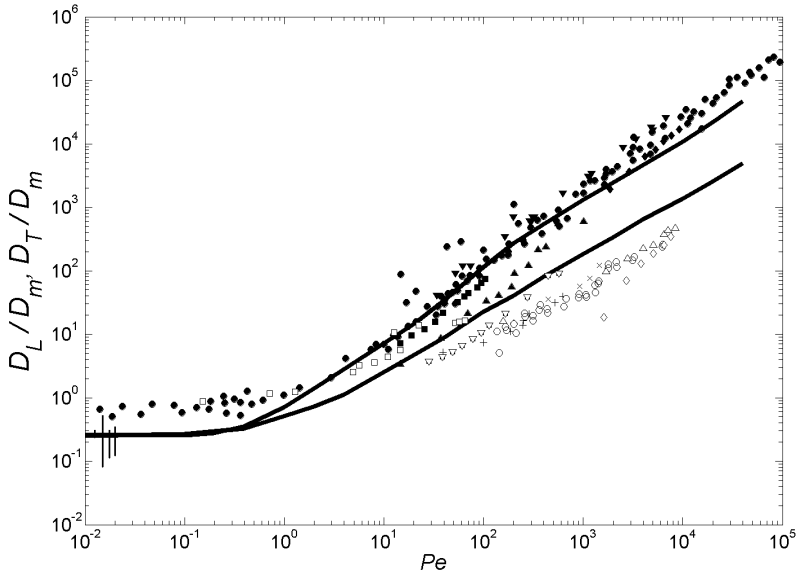

Fig. 2 Comparison of the network model results for longitudinal (upper solid line) and transverse (lower solid line) dispersion coefficients with experimental data (filled symbols for longitudinal dispersion and open symbols for transverse dispersion). The literature sources for the experimental data are given in the text. The sandstone data are presented in the far left side of the figure by the solid lines with error bars.

The magnitude of transverse dispersion is much smaller than the longitudinal dispersion and the power-law coefficient to fit $D_T \sim Pe^{\delta_T}$ is $\delta_T = 0.94 < \delta_L$ indicating a weaker transverse dispersion dependence on *Pe* than longitudinal dispersion. This coefficient is in good agreement with the large body of experimental data from Fig. 2 [*Harleman and Rumer*, 1963; *Gunn and Pryce*, 1969 and *Han et al.*, 1985], as well as data on bead packs obtained by Magnetic Resonance Imaging [*Seymour and Callaghan*, 1997; *Khrapitchev and Callaghan*, 2003]. Note also that the magnitude of the transverse dispersion from the model is higher than the experimental results by a factor of about two. This could be due to the fact that the model does not take into account the spread of particles in the third dimension. This is an issue we are currently investigating. Interestingly, our model shows that for transverse dispersion the power law coefficient in the boundary layer regime slightly decreases after $Pe > 400$ ($\delta_T = 0.89$), which marks the beginning of purely advective-dominated dispersion regime. This is a feature that is not discriminated by the experiments.

3.2 Transit time probability, $\psi(t)$, dependence on *Pe*

We use the network model to compute the transit time probability $\psi(t)$ as a function of *Pe* and match it using Eq. (1). We estimate t_1 and t_2 in Eq. (1) using physical principles. t_1 is an average advective transit time defined by L/u, where u is the mean flow speed in the throats and L is the throat length. t_2 is the late-time cut-off governed by the time necessary for a particle to diffuse between pores, $t_2=L^2/2D_m$. In Fig. 2 we plot $\psi(\tau)$, where $\tau = t/t_1$ and $t/t_2 = 2\tau/Pe$, and compare with the match to Eq. (1) for a number of *Pe*. τ can be physically interpreted as the average number of throat lengths traveled. Eq. (1) cannot reproduce the early-time behavior that is affected by the minimum travel times, but does accurately predict

$\psi(\tau,Pe)$, for $\tau > 5$ with only a single parameter $\beta = 1.8$. We see an approximate power-law scaling regime over up to three orders of magnitude from $\tau \approx 5$ ($t=5t_1$) to $\tau = Pe/2$ ($t = t_2$). The late-time cut-off is due to transport through throats where the transit time is controlled by diffusion. With increasing Pe the late-time cut-off occurs at larger τ which results in increased dispersion. Note that $\psi(\tau)$ is fit to Eq. (1) over nine orders of magnitude.

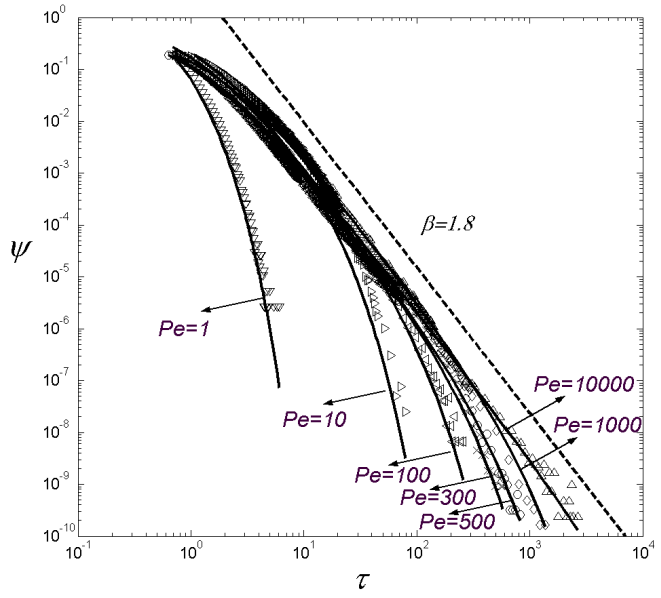

Fig. 3 The probability, ψ, of traveling between two neighboring pores in a dimensionless time $\tau = t/t_1$, where t_1 is the mean travel time L/u, plotted for different values of Pe (points). Also shown (lines) are matches using Eq. (1) with a single adjustable parameter $\beta = 1.8$. For Pe, $\tau > 5$ Eq. (1) accurately reproduces $\psi(\tau, Pe)$. To illustrate the power-law scaling a dashed line of slope $1+\beta$ is indicated on the graph.

3.3 Analysis of dispersion coefficient

Dentz et al. [2004] used Eq. (1) to derive analytically the full development of a solute plume. Here we use scaling laws to analyze the behavior as a function of Pe. In *Dentz et al.* [2004] expressions for the dispersion coefficient are written in dimensionless form $\tilde{D}$. In dimensional form $D = uL\tilde{D}$ and hence $D/D_m = Pe\,\tilde{D}$. Then for $2>\beta>1$: $D_L/D_m \sim Pe\ \tau^{2-\beta}$ while $D_T/D_m \sim Pe$ for $t_2/t_1 > \tau >> 1$. Note that D_L is a function of dimensionless time, τ, in the pre-asymptotic regime. For $\tau > \tau_{max} = ct_2/t_1$, where c is a Pe-independent prefactor greater than 1 whose value depends on the heterogeneity of the porous medium, D_L reaches its asymptotic value, $D_L/D_m \sim Pe\ \tau_{max}^{2-\beta}$ [*Dentz et al.*, 2004]. $c \approx 20$ in our simulations; the solute must experience flow through several slow-flowing regions before the average behavior is Gaussian. Hence for $Pe^{crit} > Pe >> 1$, we take $\tau_{max} = ct_2/t_1 = cPe/2$ in the expressions above and $D_L/D_m \sim Pe^{3-\beta}$ (ignoring the Pe-independent prefactor). For $Pe > Pe^{crit}$ the dispersion behavior becomes advection-controlled and in this regime $\tau_{max} = cPe^{crit}/2$ and is approximately independent of Pe. This gives $D_L/D_m \sim Pe$. This is mechanical dispersion. $D_T/D_m \sim Pe$ for all

Pe >>1. Note that this analysis fits the experimental observations and the network model predictions, Figs. 2 and 3, using $\beta = 1.8$ and hence $\delta_L = 3-\beta = 1.2$ [*Bijeljic and Blunt,* 2006].

4. CONCLUSIONS

Our network model can successfully predict asymptotic macroscopic dispersion coefficients in porous media over a broad range of Peclet numbers, $0 < Pe < 10^5$. The model is able to clearly distinguish all dispersion regimes (restricted diffusion, transition, boundary-layer and mechanical dispersion regimes) for both longitudinal and transverse dispersion.

The behavior associated with the spreading of solute in a porous medium has a simple physical explanation: the heterogeneity of the pore space leads to a variation in typical flow speeds, leading, when advection dominates at the pore scale – Pe >>1 – to an approximately power-law distribution of pore-to-pore travel times. The exponent β is related to the heterogeneity of the medium – more heterogeneous media will have a lower value of β. Dispersion is controlled by transport in throats with low velocities whose local Peclet numbers are small and hence where movement is diffusion controlled for $Pe < Pe^{crit}$. For $Pe > Pe^{crit}$, the effect of diffusion is confined to very few throats and dispersion is largely mechanical with $D_L \sim Pe$. Our demonstration that the power-law dependence of dispersion coefficient on Pe is due to the distribution of flow speeds between throats contrasts with the traditional theories of *Saffman* (1959) and *Koch and Brady* (1985) that emphasize diffusion near the solid walls within pores or at pore junctions.

Acknowledgments. We would like to thank the Engineering and Physical Sciences Research Council (EPSRC) for financial support under grant EP/C536754/1.

REFERENCES

Bear, J. (1988), *Dynamics of Fluids in Porous Media*, Elsevier Sci., Dover, New York.

Berkowitz, B., and H. Scher (1995), On characterization of anomalous dispersion in porous and fractured media, *Water Resour. Res., 31,* 1461-1466.

Berkowitz, B., H. Scher and S. E. Silliman (2000), Anomalous transport in laboratory-scale, heterogeneous porous media, *Water Resour. Res.*, *36*, 149-158.

Bijeljic, B., A. H. Muggeridge and M. J. Blunt (2004), Pore-sale modeling of longitudinal dispersion, *Water Resour. Res.*, *40*, W11501, doi:10.1029/2004WR003567.

Bijeljic, B., and M. J. Blunt (2006), Pore-scale modeling and continuous time random walk analysis of dispersion in porous media, *Water Resour. Res.*, *42*, W01202, doi:10.1029/2005WR004578.

Dentz, M., A. Cortis, H. Scher and B. Berkowitz (2004), Time behavior of solute transport in heterogeneous media: transition from anomalous to normal transport, *Adv. Water Resour., 27*, 155-173.

Dullien, F. A. L. (1992), *Porous Media: Fluid Transport and Pore Structure*, Academic Press, San Diego.

Fried, J. J., and M. A. Combarnous (1971), Dispersion in porous media, *Adv. Hydrosci.* **7**, 169-282.

Frosch, G. P., J. E. Tillich, R. Haselmeier, M. Holz and E. Althaus (2000), Probing the pore space of geothermal reservoir sandstones by Nuclear Magnetic Resonance, *Geothermics,* 29, 671-687.

Gelhar, L.W., C. Welty and K. R. Rehfelt, (1992) A critical-review of data on field-scale dispersion in aquifers, *Water Resour. Res.*, *28*, 1955-1974.

Gist, G. A., A. H. Thompson, A. J. Katz and R. L. Higgins (1990), Hydrodynamic dispersion and pore geometry in consolidated rock, *Phys. Fluids A,* 2, 1533-1544.

Gunn, D. J., and C. Pryce (1969), Dispersion in packed beds, Trans. Inst. Chem. Eng., 47, T341-T350.

Han, N.-W., J. Bhakta and R. G. Carbonell (1985), Longitudinal and lateral dispersion in packed beds: effect of column length and particle size distribution, *AIChE Journal*, *31*, 277-287.

Harleman, D. R. F. and R. R. Rumer (1963), Longitudinal and lateral dispersion in an isotropic porous medium, *J. Fluid Mech.*, 16, 385-394.

Hassinger, R. C. and D. U. von Rosenberg (1968), A mathematical and experimental examination of transverse dispersion coefficients, *SPE Journal*, 243, 195-204.

Kandhai, D., D. Hlushkou, A. G. Hoekstra, P. M. A. Sloot, H. Van As and U. Tallarek (2002), Influence of stagnant zones on transient and asymptotic dispersion in macroscopically homogeneous porous media, *Phys. Rev. Lett.*, *88*, 234501, doi: 10.1103 /PhysRevLett.88. 234501.

Khrapitchev, A. A., and P. T. Callaghan, (2003), Reversible and irreversible dispersion in a porous medium, *Phys. Fluids, 15*, 2649-2660.

Koch, D. L., and J. F. Brady (1985), Dispersion in fixed beds, *J. Fluid Mech., 154*, 399-427.

Koch, D. L., and J. F. Brady (1987), A non-local description of advection-diffusion with application to dispersion in porous media*, J. Fluid Mech., 180*, 387-403.

Legatski, M. W., and D. L. Katz (1967), Dispersion coefficients for gases flowing in consolidated porous media, *SPE Journal,* 7, 43-53.

Levy, M., and B. Berkowitz (2003), Measurement and analysis of non-Fickian dispersion in heterogeneous porous media, *J. Contam. Hydrol.*, *64*, 203-226.

Øren, P. E., and S. Bakke (2002), Process based reconstruction of sandstones and prediction of transport properties**,** *Transp. Porous Media, 46*, 311-343.

Pfannkuch, H. O. (1963), Contribution a l' etude des deplacements de fluiedes miscibles dans un milieu poreux, *Rev. Inst. Fr. Petrole, 18*, 215-270.

Saffman, P. G. (1959), A theory of dispersion in a porous medium, *J. Fluid Mech., 6*, 321-349.

Sahimi, M. (1995), *Flow and Transport in Porous Media and Fractured rock: From Classical Methods to Modern Approaches*, VCH, Cambridge, Weinheim.

Scher, H., and M. Lax (1973), Stochastic transport in a disordered solid. I. Theory, *Phys. Rev. B*, *7*, 4491-4502.

Seymour, J. D., and P. T. Callaghan (1997), Generalized approach to NMR analysis of flow and dispersion in porous media, *AIChE Journal,*.43,. 2096-2111.

Stöhr, M. (2003), Analysis of flow and transport in refractive index matched porous media, PhD Thesis, Univ. of Heidelberg, Heidelberg, Germany.